Supporting Information

Theoretical Prediction of Two-Dimensional SnP_3 as a Promising Anode Material for Na-Ion Batteries

Chun-Sheng Liu, Xiao-Le Yang, Jin Liu, and Xiao-Juan Ye*

Key Laboratory of Radio Frequency and Micro-Nano Electronics of Jiangsu Province, College of Electronic and Optical Engineering, Nanjing University of Posts and Telecommunications, Nanjing 210023, China

* E-mail: yexj@njupt.edu.cn

I. Methods for optical properties and Fukui function calculations

To calculate the optical properties of monolayer SnP_3, the absorption coefficient is determined by the dielectric functions, which is obtained by the following equation:[1]

$$\alpha(\omega) = \sqrt{2}(\omega)[\sqrt{\varepsilon_1^2(\omega) + \varepsilon_2^2(\omega)} - \varepsilon_1(\omega)]^{1/2}$$

where the real part of the dielectric function $\varepsilon_1(\omega)$ is derived from the Kramers-Kronig transformation and the $\varepsilon_2(\omega)$ is computed by summation over empty states. According to the above components of the absorption spectra, the optical properties can be determined. The Fukui function provides the information about a highly electrophilic/nucleophilic center in a system.[2] The condensed Fukui function f_κ^+ for nucleophilic attack, f_κ^- for electrophilic attack, and f_κ^0 for free radical attack can be defined as:

for nucleophilic attack $f_\kappa^+ = [q_\kappa(N+1) - q_\kappa(N)]$

for electrophilic attack $f_\kappa^- = [q_\kappa(N) - q_\kappa(N-1)]$

for free radical attack $f_\kappa^0 = [q_\kappa(N+1) - q_\kappa(N-1)]/2$

where q_k represents the electronic population of atom k in the cationic (*N*-1), neutral (*N*) or anionic (*N*+1) chemical species.

II. The structure properties of SnP_3

The calculated atomic positions for the optimized SnP_3 monolayer with the lattice constants a=b=7.166 Å and c=30 Å**.** The bond angles are α=89.991°, β=90.009°, and γ=119.997°.

	x	y	z
P1	1.790263477	-1.033696065	15.531275638
P2	-0.002016857	2.070643538	15.530505266
P3	-1.794314763	-1.033494061	15.530507396
P4	-1.794904277	1.036341937	14.871533998
P5	1.789967438	1.035624720	14.869593907
P6	-0.002031033	-2.067995438	14.869596359
Sn1	3.579471577	2.071078560	16.611656381
Sn2	-0.002069975	4.139027698	13.789341273

Table S1. Calculated lattice parameters C (Å), bond lengths L (Å), and bond angles θ (°) of bulk and mono-layered SnP_3.

Structure	$C_{a=b}$	C_c	$L_{p\text{-}p}$	$L_{Sn\text{-}p}$	$\theta_{p\text{-}p\text{-}p}$	$\theta_{p\text{-}Sn\text{-}p}$	$\theta_{Sn\text{-}p\text{-}p}$
Experimental bulk SnP_3[3]	7.378	10.512	2.223	2.662	99.049	97.301	98.184
bulk SnP_3	7.338	10.686	2.229	2.639	99.853	96.161	98.049
monolayer SnP_3	7.166	/	2.172	2.704	111.205	82.983	99.642

III. In-plane stiffness (C_{2D})

In order to calculate the in-plane stiffness along the armchair and zigzag directions, a rectangle lattice is used as shown in Figure S1a. The C_{2D} is defined as $(E - E_0)/S_0 = C_{2D}(\Delta l/l_0)^2/2$, where E_0 is the total energy of cell without strain and S_0 is the equilibrium lattice area. The strain step of this data calculation is 0.5%. Here, the l_0 is the lattice constant along the transport direction, and Δl is the deformation of l_0. The relationship between $\Delta E = E - E_0$ and $\Delta l/l_0$ is shown in Figure S1b. The in-plane stiffness C_{2D} of monolayer SnP_3 is 31.62 (31.53) N/m along the zigzag (armchair) direction.

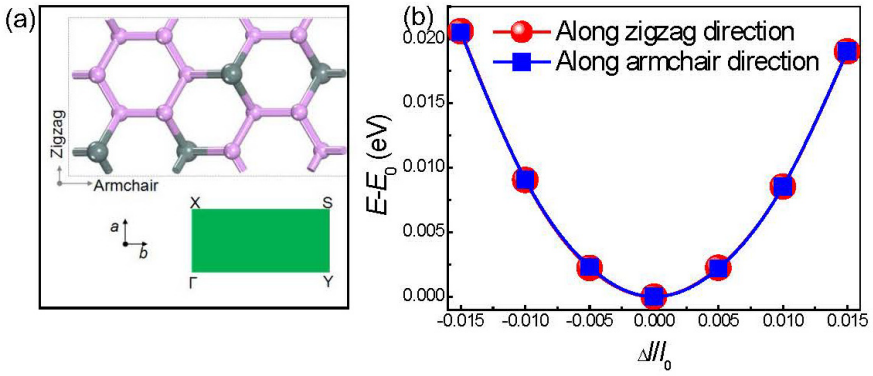

Figure S1. (a) Monolayer SnP_3 in a rectangle super cell. The green region represents the Brillouin zone of monolayer SnP_3. (b) The total energy E-E_0 shift as a function of the lattice strain along zigzag and armchair directions of monolayer SnP_3.

IV. AIMD simulations

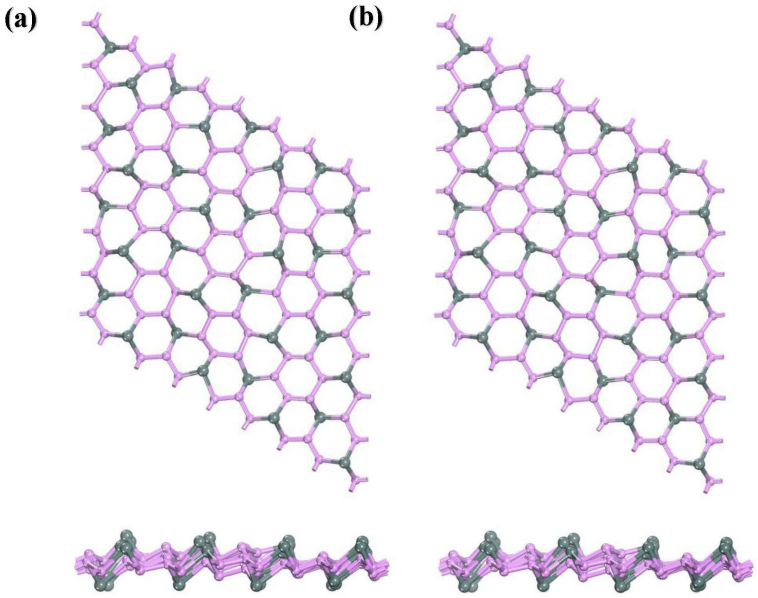

Figure S2. Top and side views of the snapshot of monolayer SnP_3 at T=300 (a) and 600 K (b) (P and Sn atoms are denoted by the small and large balls, respectively).

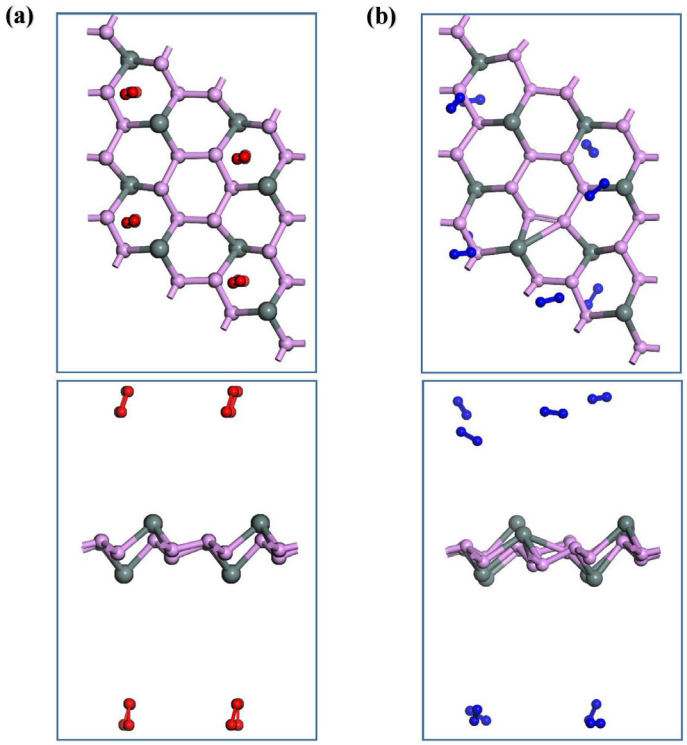

Figure S3. AIMD snapshots of monolayer SnP_3 exposed to the (a) oxygen and (b) nitrogen molecules at 600 K.

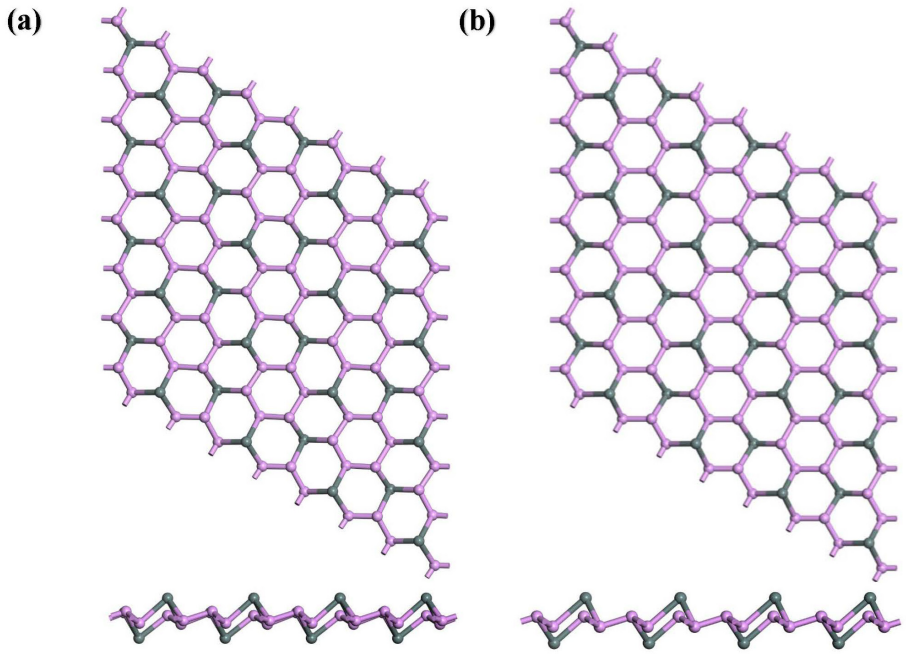

Figure S4. AIMD snapshots of monolayer SnP_3 in the (a) ethyl methyl carbonate and (b) dimethyl carbonate solvation models at 300 K.

V. The band structures of multilayer SnP_3

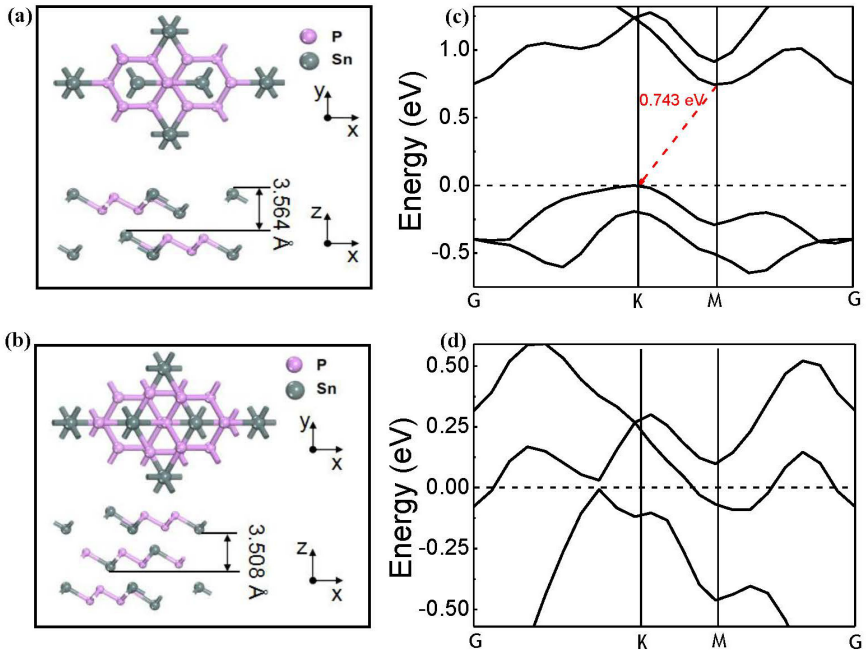

Figure S5. Top and side views of (a) bilayer and (b) trilayer SnP_3 with respect to the band structures (c) and (d), respectively. Dashed line at 0 eV denotes the Fermi level.

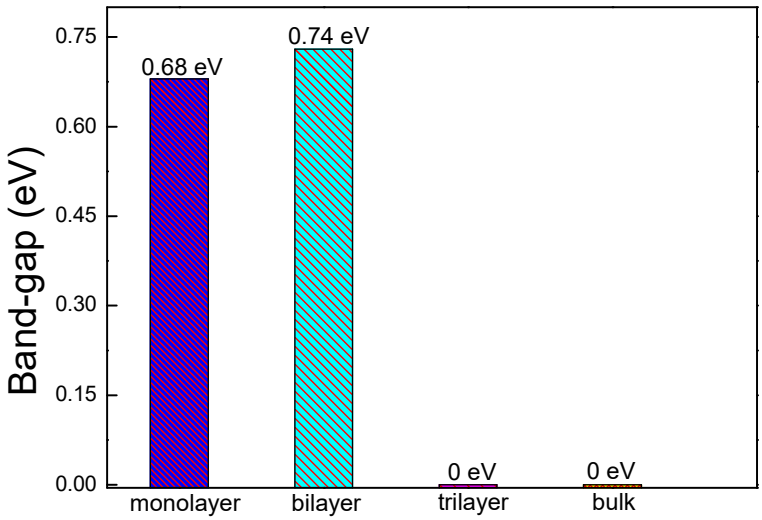

Figure S6. The band-gap values (at the HSE06 level) of SnP_3 with different layers.

VI. The charge density difference of monolayer SnP_3

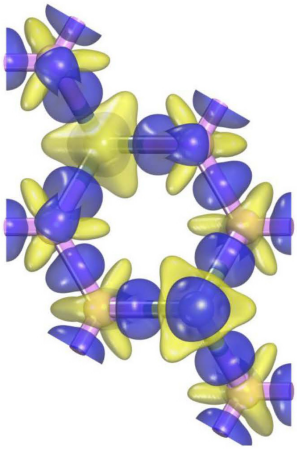

Figure S7. The charge density difference plot of the pristine SnP_3 monolayer. The yellow and blue areas represent the electron depletion and accumulation regions, respectively. The iso-surface value is 0.05 eÅ^{-3}.

VII. The band structures of monolayer SnP_3 under biaxial strain

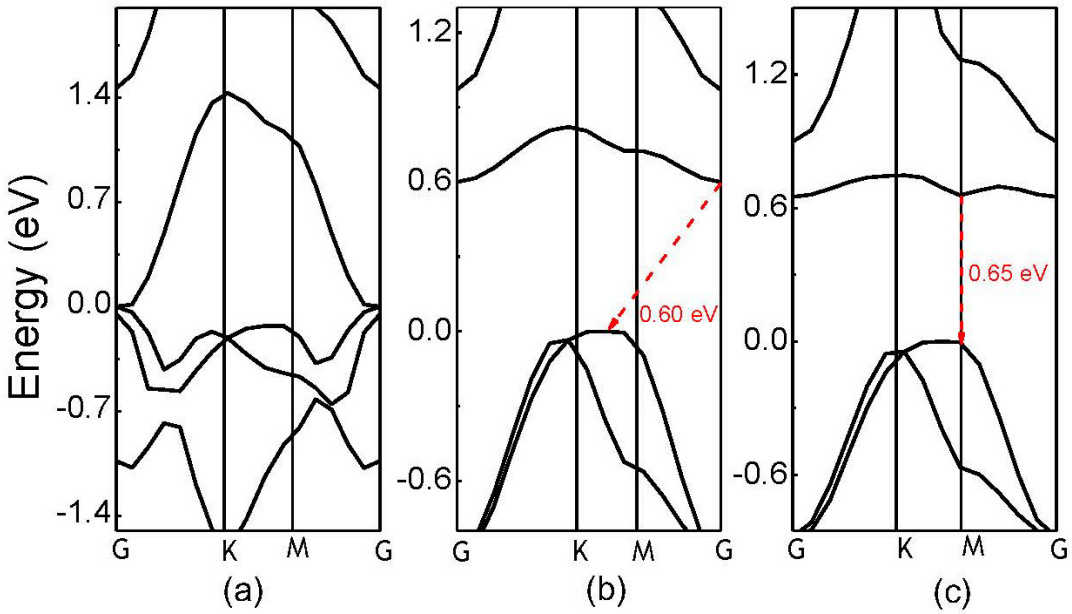

Figure S8. Electronic band structures of monolayer SnP_3 under -0.06 (a), 0.06 (b), and 0.08 (c) biaxial strain.

VIII. Carrier mobility

According to the deformation potential (DP) theory,[4] the carrier mobility of 2D materials can be estimated by the following expression:

$$\mu = \frac{e\hbar^3 C_{2D}}{K_B T m_i^* m_d (E_1^i)^2}$$

where $\hbar$, K_B, T, and m^* are the reduced Planck constant, Boltzmann constant, temperature (300 K), and effective mass, respectively. m_i^*(i = h for holes, i = e for electrons) is based on the effective mass approximation $m^* = \hbar^2(\partial^2 E/\partial K^2)^{-1}$. The effective masses along the a (b) direction are 0.32 (0.38) m_0 for electron and 1.08 (0.23) m_0 for hole. The average effective mass m_d is determined by $m_d = \sqrt{m_x^* m_y^*}$. The deformation potential constant E_1 is defined by $\frac{\Delta V}{\Delta l / l_0}$, which represents the energy of CBM for electrons and the VBM for holes along the transport (a and b) direction. ΔV is the energy change (conduction band or valence band) under certain strain. The relationship between E_1 and dilation $\Delta l/l_0$ is shown in Figure S9b. The deformation potentials (E_1) of SnP_3 monolayer are 0.93 (0.93) eV for electron and 1.68 (0.62) eV for hole along the zigzag (armchair) direction, respectively.

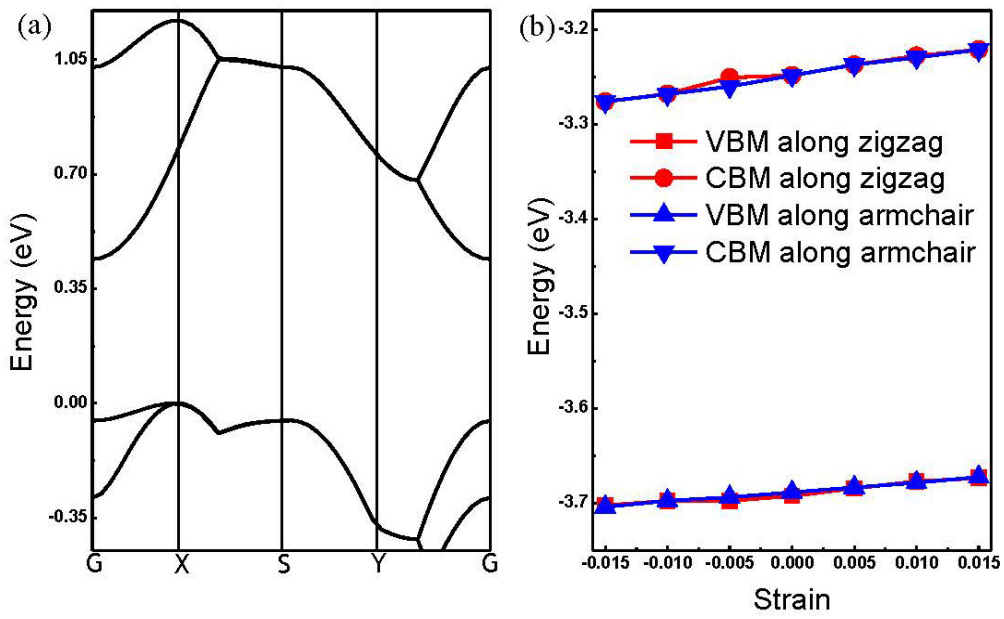

Figure. S9 (a) The band structure for monolayer SnP_3 in an orthogonal lattice. (b) Energy shift of VBM and CBM with respect to the lattice dilation and compression along zigzag and armchair directions.

IX. Na adsorption sites and PDOS

(a) site 1: the top of a Sn1 atom of Sn_2P_4 hexagonal honeycomb configuration; (b) site 2: above the top of a Sn2 atom; (c) site 3: over the hollow of the P_6 hexagon; (d) site 4: above the top of a P1 atom; (e) site 5: above the top of P2 atom; and (f) site 6: over the center of P_6 hexagonal hollow.

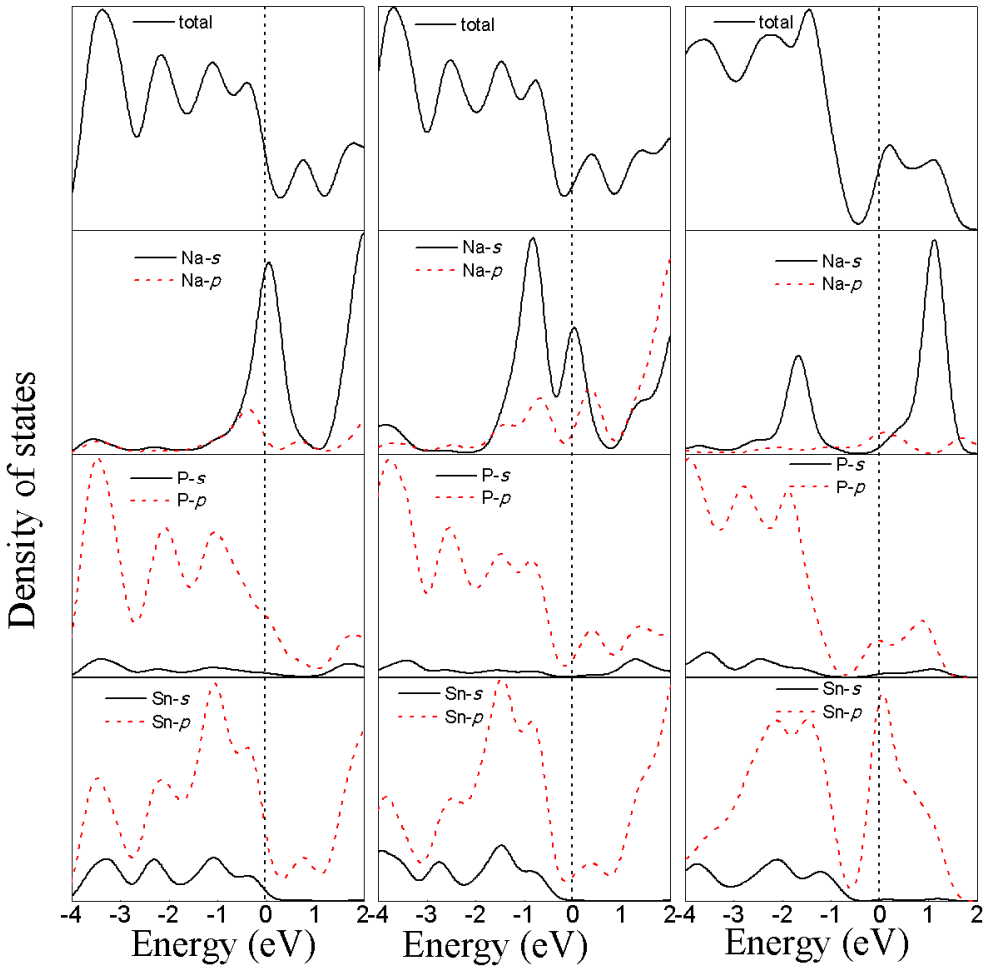

Figure S10. The total and partial density of states of Na adsorbed site 2 (a) and site 4 (b) on the SnP_3 monolayer. (c) The total and partial density of states of Na-bilayer SnP_3. The Femi levels have been shifted to zero.

Table S2. Calculated changes in the lattice parameters and volume during the sodiation/desodiation process.

Bulk	*a* (Å)	*b* (Å)	*c* (Å)	Volume (Å^3)	Volume (Å^3) ($Sn_{48}P_{144}$)	V/V_{SnP_3}
SnP_3 (Sn_6P_{18})	7.44	7.44	10.41	499.03	3992.24	1.0
Na_3P (Na_6P_2)	4.51	4.51	8.04	141.62	10196.64	2.55
$Na_{15}Sn_4$($Na_{60}Sn_{16}$)	12.71	12.71	12.71	2053.23	6159.69	1.54

Reference

(1) Saha, S.; Sinha, T.; Mookerjee, A. Electronic Structure, Chemical Bonding, and

Optical Properties of Paraelectric $BaTiO_3$. *Phys. Rev. B* **2000**, *62*, 8828.

(2) Yang, W.; Mortier, W. J. The Use of Global and Local Molecular Parameters for the Analysis of the Gas-Phase Basicity of Amines. *J. Am. Chem. Soc.* **1986**, *108*, 5708-5711.

(3) Gullman, J.; Olofsson, O. The Crystal Structure of SnP_3 and a Note on the Crystal Structure of GeP_3. *J. Solid State Chem*. **1972**, *5*, 441-445.

(4) Barden, J.; Shockley, W. Deformation Potentials and Mobilities in Non-Polar Crystals. *Phys. Rev.* **1950**, *80*, 72–80.